

This is a provisional PDF only. Copyedited and fully formatted version will be made available soon.

Authors: Oksana Nakonechna, Galina Gubina-Vakulick, Valeriy Miasoiedov, Tatyana Gorbach, Svitlana Denysenko, Svitlana Yefimova, Vladimir Klochkov, Svitlana Stetsenko, Irina Vasylyeva, Daria Yankovska

Article type: Original Article

Received: 12 June 2025

Accepted: 26 October 2025

Published online: 7 January 2026

eISSN: 2544-1361

Eur J Clin Exp Med

doi:10.15584/ejcem.2026.1.16

This is a PDF file of an unedited manuscript that has been accepted for publication. As a service to our authors we are providing this early version of the manuscript. The manuscript will undergo copyediting and typesetting. Please note that during the production process errors may be discovered which could affect the content, and all legal disclaimers that apply to the journal pertain.

Identification of hepatotoxicity of untreated and UV-irradiated GdYVO₄:Eu³⁺ nanoparticles

Oksana Nakonechna¹, Galina Gubina-Vakulick², Valeriy Miasoiedov³, Tatyana Gorbach¹, Svitlana Denysenko¹, Svitlana Yefimova⁴, Vladimir Klochkov⁴, Svitlana Stetsenko¹, Irina Vasylyeva¹, Daria Yankovska⁵

¹ Department of Biochemistry, Kharkiv National Medical University, Kharkiv, Ukraine

² Department of Pathological Anatomy, Kharkiv National Medical University, Kharkiv, Ukraine

³ Department of Medical Biology, Kharkiv National Medical University, Kharkiv, Ukraine

⁴ Institute of Scintillation Materials, NAS of Ukraine, Kharkiv, Ukraine

⁵ Research Institute of Experimental and Clinical Medicine, Kharkiv National Medical University, Kharkiv, Ukraine

Corresponding author: Svitlana Denysenko, e-mail: sa.denysenko@knmu.edu.ua

ORCID

ON: <https://orcid.org/0000-0002-2614-1587>

GG-V: <https://orcid.org/0000-0003-3816-8530>

VM: <https://orcid.org/0000-0001-7135-4672>

TG: <https://orcid.org/0000-0003-4819-7220>

SD: <https://orcid.org/0000-0002-8457-4436>

SY: <https://orcid.org/0000-0003-2092-1950>

VK: <https://orcid.org/0000-0002-8080-1195>

SS: <https://orcid.org/0000-0003-2783-2694>

IV: <https://orcid.org/0000-0002-4475-167X>

DY: <https://orcid.org/0009-0002-2538-4867>

ABSTRACT

Introduction and aim. Gadolinium–yttrium orthovanadate GdYVO₄:Eu³⁺ nanoparticles (NPs) display dual redox activity, acting as pro-oxidants or antioxidants depending on the surrounding environment, concentration, and pretreatment conditions, a property that can be harnessed for potential oncological therapies. This study aims to evaluate the effect of untreated and UV-irradiated NPs administered orally on blood biochemical parameters, liver tissue, and histological condition of liver tissue in an experiment on laboratory rats.

Material and methods. Male rats of the WAG population received oral colloidal NPs solutions (in untreated and UV-irradiated forms) at different doses: (50, 100, 200) $\mu\text{g}/\text{kg}$ of body weight for 14 days. The content of medium-weight molecules, alanine aminotransferase activity, direct and indirect bilirubin content, and von Willebrand factor content were determined in blood serum. The content of reduced glutathione, superoxide dismutase, diene conjugates, and TBK-active products was determined in liver homogenates. Liver tissue samples were examined using morphological and morphometric methods.

Results. The formation of oxidative stress, intoxication, damage to endothelial cells, impaired membrane permeability, destruction of hepatocytes, and destruction of sinusoidal endothelial cells were detected.

Conclusion. It has been established that the introduction of GdYVO₄: Eu³⁺ NP, both in untreated and UV-irradiated forms, induces dose-dependent effects, including oxidative stress, endothelial dysfunction, intoxication, damage to hepatocyte membranes, functional and histological damage to the liver, with more pronounced effects observed for UV-irradiated NPs.

Keywords. gadolinium-yttrium orthovanadate nanoparticles, hepatotoxicity, oxidative stress, UV-irradiation

Introduction

Scientific progress in chemistry and physics has opened new avenues in the field of nanobiotechnology, enabling the synthesis of specific nanoparticles (NP) and their widespread use in medical applications for the therapy and diagnosis of various serious diseases, particularly cancer.¹ The utilization of nanomaterials holds promise for targeted drug delivery to specific organs, early diagnosis, and treatment of oncologic diseases, as well as coating of surgical instruments and implants with nanoparticles, and the development of new antimicrobial agents, vaccines, and drugs.²

Despite the advancements, the impact of synthesized NPs on living organisms remains insufficiently studied. In recent years, there has been growing scientific interest in inorganic nanomaterials based on rare-earth metals.³⁻⁴ The colloidal solutions of these materials exhibit luminescence, offering an expanded capability to monitor biochemical processes.⁵ Currently, stable gadolinium compounds are commonly used as magnetic resonance contrast agents, serving as radiosensitizers in radiation therapy of oncological diseases.⁶ NPs with rare-earth (RE) ions have unique optical properties and biocompatibility,⁷ high photostability, absence of flicker effect, narrow emission lines, and prolonged luminescence.⁸ This makes it possible to use such NPs for DNA detection, protein detection of proteins and study of their interactions, imaging in vivo and in vitro.⁷ It has been shown that NPs can be used to increase the efficiency of chemotherapy.⁹ Complexes based on rare-earth metals are used in gene therapy.¹⁰⁻¹² It was found that many complexes of rare earth metals based on inorganic compounds have antiproliferative,¹³ antibacterial¹⁴ anti-inflammatory¹⁵ properties. Tkachenko and his coauthors showed that GdYVO₄: Eu³⁺ NP prevent the development of carrageenan-induced intestinal inflammation.¹⁶ REVO₄:Eu³⁺ (RE=Gd,Y,La) nanoparticles

were found to have antioxidant properties.¹⁶⁻¹⁷ At the same time, there are works showing that REVO4: Eu³⁺ NP exhibit pro-oxidant properties and inhibit enzymes of the antioxidant system (AOS).¹⁸⁻²⁰ It was found that gadolinium-based nanocomplexes can accumulate in tumor tissues and increase their sensitivity to radiation therapy.²¹ At the same time, a number of authors note the presence of negative consequences of the use of gadolinium NP as contrast materials. The authors pay special attention to pathological consequences in brain, kidney, skin, and bone tissues, and to the development of general hypersensitivity reactions.²² Taking into account the promising application of nanoparticles with RE ions, it should be taken into account that colloidal solutions of nanoparticles themselves can exhibit biological activity. They have unique physical and chemical properties and are characterized by a wide spectrum of biological action.²³ Their effect on living organisms, including toxic effects, is due, as a rule, to the high chemical and catalytic activity of the specific surface area of NPs, which is insignificant in particles of the same nature but of larger size in most cases.²⁴ Due to their small size, NPs are able to penetrate through the skin, digestive and respiratory systems and accumulate in cells of organs and tissues. The interaction of NPs with proteins is considered; the resulting complex can induce conformational changes in protein molecules.²⁵⁻²⁶ GdYVO₄:Eu³⁺ NPs are characterized by unique redox flexibility: depending on external conditions, they can promote or suppress the formation of reactive oxygen species (ROS). UV pretreatment was shown to shift their activity from antioxidant to pro-oxidant, highlighting its potential for redox-modulating biomedical applications.²⁷⁻²⁸ This property of GdYVO₄:Eu³⁺ that provides the prospect of their application in medicine, in particular oncology. In *in vitro* experiments, activated GdYVO₄: Eu³⁺ NP was shown to induce the development of oxidative stress in leukocytes, leading to increased generation of ROS and activation of apoptosis.²⁸ This feature of action may be key in the treatment of cancer, but in other diseases may cause the development of fibrosis.²⁹ The probability of the development of pathologic conditions caused by the use of nanomaterials is quite real, so the elucidation of the causes of the toxic action of NPs is now becoming the subject of a new direction in experimental medicine.³⁰ In many world studies, the analysis of developing toxic damage was carried out taking into account normal or decompensated kidney function in patients (or experimental animals), since the excretion of these substances from the body is carried out mainly through the kidneys. In cases of problematic excretion of gadolinium-containing contrast agent through the kidneys, gadolinium accumulated in tissues. The name of such a pathological condition Gadolinium deposition disease was suggested.²⁰ Current sources of scientific literature do not contain enough information; at the same time, such studies are necessary, since the accumulation of NP in the liver after their administration into the blood is significant.

Aim

The aim of this work is to evaluate the possibility of its hepatotoxic effect on the biochemical parameters of blood, liver homogenates, and the liver histological state in laboratory rats based on in vivo study of the cumulative effect of untreated and UV-irradiated GdYVO₄:Eu³⁺ nanoparticles in different concentrations.

Material and methods

The GdYVO₄: Eu³⁺ (GdYVO) nanoparticles were supplied by the Institute of Scintillation Materials of the National Academy of Sciences of Ukraine under a cooperation agreement with Kharkiv National Medical University (No. 173/09-19n). GdYVO NPs were synthesized by a previously described method³¹ and provided as colloidal aqueous solutions containing 1 g/L of solid phase, consisting of nearly spherical particles with an average diameter of ~2 nm. To minimize possible toxic effects, the substance was administered in small doses of 50, 100, and 200 µg/kg body weight for 14 days. Nonirradiated and UV irradiated GdYVO NPs were administered (immediately before administration to rats, GdYVO NP was activated by training for 20 min with UV light, in a quartz cuvette at a distance of 20 cm from the irradiation source, using a UV irradiation source of "Quartz-125" type, ($\lambda=210-400$ nm) according to the method described previously.²⁷⁻²⁸ The substance was administered orally using automatic dosing.

Animal groups

The experiments were carried out in male WAG rats weighing between 180 and 200 g, housed in standard vivarium conditions with natural light and provided with a balanced diet. The rats were randomly assigned to seven groups, each consisting of six individuals.

1. Control group (Gr. C1):

Orally received 0.18-0.20 ml of drinking water.

2. Experimental group 2 (EG-50):

Received a solution of GdYVO NP at a dose of 50 µg/kg body weight.

3. Experimental group 3 (EG-100):

Received a GdYVO NP solution at a dose of 100 µg/kg body weight.

4. Experimental group 4 (EG-200):

Received a GdYVO NP solution at a dose of 200 µg/kg body weight.

5. Experimental group 5 (EGA-50):

Received a solution of UV-activated GdYVO NPs at a dose of 50 µg/kg body weight.

6. Experimental group 6 (EGA-100):

Received a solution of UV-activated GdYVO NPs at a dose of 100 µg/kg body weight.

7. Experimental group 7 (EGA-200):

Received a solution of UV-activated GdYVO NPs at a dose of 200 µg/kg body weight.

This ensures clarity about the nature of the GdYVO NPs in each group, indicating whether it were untreated or UV-activated.

Material collection

At the end of the administration of GdYVO NP solution administration on the next day, rats were removed from the experiment by decapitation using a guillotine, blood was collected, and the liver was isolated at autopsy. The liver suspension (approximately 300 mg) was ground with scissors in a mortar on ice, then saline was added (at the rate of 10 ml of saline per 1g of tissue), homogenized in a Potter homogenizer (on ice) until a homogeneous mass was obtained. The homogenate was centrifuged at 600 g for 10 minutes (centrifuge Universal 320R). The supernatant was used for biochemical studies. Serum was obtained from blood (coagulation followed by centrifugation) and used for biochemical studies.

Another piece of liver tissue was fixed in 10% neutral formalin for morphologic studies.

When working with experimental animals, we were guided by the provisions of the European Convention for the Protection of Vertebrate Animals (Strasbourg, 18.03.1986, revised and amended in 2006), the Law of Ukraine Nos. 3447 - IV, Articles 26, 31 "On the Protection of Animals against Cruelty", "General ethical principles of experiments on animals", adopted by the Fifth National Congress on Bioethics (Kiev, 2013). The following biochemical techniques were used: - to assess the level of intoxication, the content of medium mass molecules (MMM) in blood serum was determined by the express method³² to assess the activity of lipid peroxidation (LPO), the content of diene conjugates (DC) and TBA-active products in liver homogenates. The DC content was determined according to the method described in reference 33. The DC content in the sample was expressed in mM/g protein. The concentration of TBA-active products in liver homogenates was determined using the test with 2-thiobarbituric acid according to the method of Botsoglow et al.³⁴ The content of TBA-active products was expressed in μ M/g protein; – the amount of protein in tissues was determined by the spectrophotometric method;³⁵ – the state of the antioxidant system was evaluated by the content of reduced glutathione and the content of superoxide dismutase (SOD) in liver homogenates. SOD content was determined by an immunoenzymatic method using SOD ELISA Kit, Elabscience (USA), expressed in pg/mL. Measurements were performed on a semiautomatic analyzer Stat Fax (USA). The determination of reduced glutathione was performed according to the method of Teidze³⁶ and Tupper.³⁷ The content of reduced glutathione was expressed in mM/g tissue. Measurements were performed on a Scolar PV-128 spectrophotometer; To evaluate the integrity of hepatocyte membranes, the activity of alanine aminotransferase (AlAT) in serum was determined using reagent kits from "Filisit Diagnostics" (Dnipro City, UA); – to assess liver function the content of direct (DB) and indirect (IB) bilirubin in blood serum was determined. The determination was carried out using a set of reagents from the company "Filisit Diagnostics" (Dnepr city, UA); – to assess the state of the blood vessel endothelium in experimental rats, we determined the content of Willibrandt factor (vWF) in the blood serum of rats. The

determination was carried out by immunoenzymatic method using the Elabscience VWF ELISA KIT reagent kit from Elabscience Biotechnology (USA). Measurements were made on a Stat Fax semiautomatic immunoenzyme analyzer (USA). Statistical processing of the data obtained in the studies was carried out using the Graph Pad Prism 5 program (Graph Pad Software, USA) using the non-parametric Mann-Whitney U criterion (comparison between two independent groups of variables). Results were presented as Median (Me) and interquartile interval Me [25%, 75%]. Differences at $p < 0.05$ were considered statistically significant. To determine the effect of NPs on the functional state of the liver, we performed morphological and morphometric studies. After fixation, liver pieces were subjected to paraffin embedding and 4-5 μm thick slices were stained with chromic hematoxylin-eosin and galloxyanin alum by Einarson for nucleic acids. Microscopic examination of liver micro preparations was performed using a microscope with a digital camera. Using Photoshop 13, the optical density of the cytoplasm of hepatocytes in the second zone of the acinus was determined on Einarson stained liver micrographs, which allows one to judge the content of RNA in the cytoplasm and, therefore, the level of protein synthetic function.³⁸

Results

Biochemical research

For science and practice, it is important to determine the concentrations of colloidal solution of GdYVO NPs, at which they will be safe for the body and, at the same time, capable of having a therapeutic effect. On the basis of this, we used in experiments various concentrations of colloidal solution of GdYVO NPs for oral administration, as well as their native and activated forms. The study of the content of medium molecules (MM) (a universal indicator of intoxication) showed that its level in the blood in rats of the EG-50 group, compared with the animals of the control group, does not differ statistically. The most significant difference in MM content of MM was observed at doses of 100 and 200 $\mu\text{g}/\text{kg}$. An increase in the dose of orally administered GdYVO NPs leads to a proportional increase in the content of MM, that is, an increase in the level of intoxication. The same dependence is characteristic for activated NPs (Fig.1).

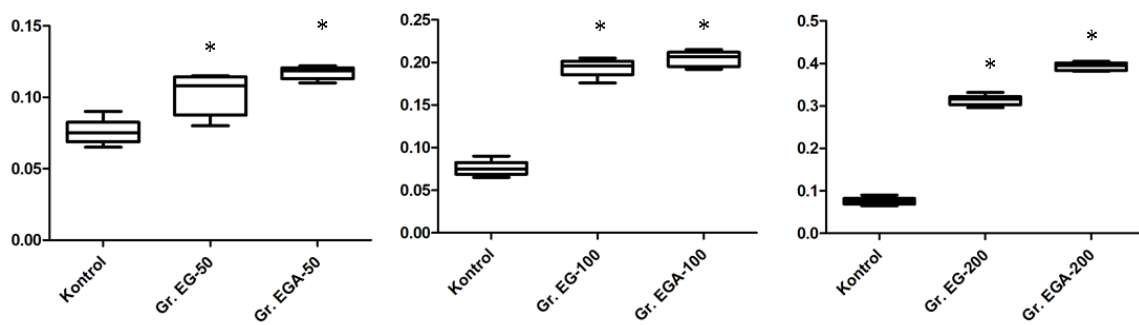


Fig. 1. Content of middle molecules (standard units) in the blood serum of rats after administration of the GdYVO4: Eu³⁺ NP solution (in untreated and UV-irradiated forms), each group compared to the control group, * p <0.05

It should be noted that the MM content in rat serum at all applied concentrations of untreated and UV-irradiated NPs is significantly higher than in the control group. Significant differences in MM content between the indices when using inactivated and activated NPs were revealed only at the dose of 200 µg/kg body weight. Consequently, oral administration of untreated and UV-irradiated GdYVO NPs to rats is accompanied by the development of intoxication, the degree of which increases with increasing dose. A higher toxicity of UV-irradiated GdYVO NP, compared to untreated ones, was revealed only at a dose of 200 µg/kg body weight.

To assess the integrity of hepatocyte membranes under intoxication we have we studied the activity of alanine aminotransferase in blood serum of rats (Table 1).

Table 1. AIAT activity (µM/hour/mL) in blood serum during oral administration of colloidal solution of GdYVO4: Eu3 + NP, [Me (25,75)] to rats*

Indicator	Gr.Cl	Gr. EG-50	Gr.	Gr.	Gr.	Gr.	Gr.
		EGA-50	EG-100	EGA-100	EG-200	EGA-200	
AIAT	0.135 [0.119;0.153]	0.109 [0.087;0.115]	0.150 p ₁ =0,0057	0.223 0.168]	0.275 0.220]	0.315 0.293]	0.355 0.550]
			p ₁ =0.0305	p ₁ =0.0022	p ₁ =0.0022	p ₁ =0.0022	p ₁ =0.0022
			p ₂ =0.0067		p ₂ =0.0043		p ₁ =0.0034

*AIAT – alanine aminotransferase, p1 – probability of differences between control and experimental groups, p2 – probability of differences between native and activated groups within one dose

As can be seen from the data given in Table 1, at oral administration of colloidal solution of untreated GdYVO NPs at a dose of 50 µg/kg, the activity of AIAT is even lower than in the control group. In case of administration of UV-irradiated GdYVO NPs, AIAT activity is, slightly higher, and there is an insignificant change in membrane permeability. When rats received a dose of 100 µg/kg, there was a significant increase in serum ALAT activity in serum both in the case of untreated and UV-irradiated GdYVO NP, and in the case of UV-irradiated NP to a greater extent. Changes of the same nature, but more pronounced, occur with oral administration of GdYVO NP at a dose of 200 µg/kg. Consequently, at doses of 100 and 200 µg/kg there is a significant dose-dependent change in permeability of the hepatocyte membrane. The study of the concentration of lipid peroxidation (LPO) products in the liver homogenates

of experimental rats showed that in the EG-50 and EG-100 the content of DC increased significantly and in the corresponding groups EGA-50 and EGA-100 the degree of increase is even greater (Table 2). As can be seen from the data given in the table, the higher the administered dose of GdYVO NPs, the greater the index value.

Table 2. Content of DC and TBA active products in liver tissue homogenates in rats during oral administration of a colloidal solution of GdYVO4: Eu³⁺ NP (in untreated and UV-irradiated forms), [Me (25, 75)]*

Groups/Indicators	DC, mM/g protein	TBA-active products, μ M/g protein
Gr. Cl	58.71 [58.54; 60.88]	26.63 [24.32;27.22]
Gr. EG-50	62.01 [60.39; 62.85] $p_1=0.0260$	27.35 [26.78; 28.12] $p_1=0.0047$
Gr. EGA-50	65.93 [64.97; 66.91] $p_1=0.0022$ $p_2=0.0024$	28.34 [27.39; 28.75] $p_1=0.0032$ $p_2=0.0028$
Gr. EG-100	74.43 [72.00; 75.46] $p_1=0.0023$	31.12 [29.88; 32.25] $p_1=0.0035$
Gr. EGA-100	79.02 [76.38; 80,50] $p_1=0.0022$ $p_2=0.0043$	32.36 [32.07; 32.86] $p_1=0.0029$ $p_2=0.0021$
Gr. EG-200	90.85 [89.17; 91.70] $p_1=0.0022$	36.45 [36.12; 37.03] $p_1=0.0024$
Gr. EGA-200	98.15 [96.35; 99.79] $p_1=0.0022$ $p_2=0.0022$	38.42 [37.94; 38.66] $p_1=0.0039$ $p_2=0.0121$

* DC – diene conjugates, p_1 – probability of differences between control and experimental groups, p_2 – probability of differences between native and activated groups within one dose

As can be seen from the data in Table 2, the rats of EG-200 and EGA-200 groups have the highest content of DC in liver homogenates among all groups. We also can say that the level of increase in DC concentration in general is higher with introduction UV-irradiated GdYVO NPs, even among lower administered concentrations. Analysis of the the content of end products of the active products of lipid peroxidation TBA showed that their concentration in liver homogenates changes significantly (but reliably) changes in rats of

the EG-50 and increases EGA-50 groups, and significantly increases in the EG-100 and EGA-100 groups and to the greatest extent in rats of the EG-200 and EGA-200 groups (Table 2).

As can be seen from the data obtained by us, at the introduction of UV-irradiated GdYVO NPs the degree of increase in the concentration of end products of LPO is higher than that at the introduction of untreated NPs, which indicates higher pro-oxidant properties of UV-irradiated GdYVO NPs. One of the main indicators of the the state of antioxidant system is the following superoxide dismutase (SOD) (Table 3).

Table 3. Content of SOD and glutathione in liver tissue homogenates in rats during oral administration of colloidal solution of GdYVO4: Eu³⁺ NP (in untreated and UV-irradiated form) [Me (25, 75)]*

Groups/Indicators	SOD, pkg/mL	Glutathione, mM/g tissue
Gr. Cl	2.11 [1.97; 2.21]	25.73 [25.53; 25.97]
Gr. EG-50	3.75 [3.71; 3.86] p ₁ =0.0056	27.00 [26.92; 27.25] p ₁ =0.0038
Gr. EGA-50	3.82 [3.77; 3.89] p ₁ =0.0031 p ₂ =0.0502	26.48 [26.34; 26.75] p ₁ =0.0056 p ₂ =0.0347
Gr. EG-100	1.95 [1.90; 2.06] p ₁ =0.0067	23.42 [23.27; 23.56] p ₁ =0.0022
Gr. EGA-100	2.03 [1.98; 2.09] p ₁ =0.0058 p ₂ =0.0487	20.34 [20.19; 20.58] p ₁ =0.0022 p ₂ =0.0039
Gr. EG-200	0.87 [0.85; 0.91] p ₁ =0.0018	19.22 [19.13; 19.46] p ₁ =0.0019
Gr. EGA-200	0.69 [0.64; 0.73] p ₁ =0.0019 p ₂ =0.0022	16.34 [16.19; 16.57] p ₁ =0.0019 p ₂ =0.0019

* SOD – superoxide dismutase, p₁ – probability of differences between control and experimental groups, p₂ – probability of differences between the untreated and UV-irradiated groups within one dose

As can be seen from the data we received when introducing the SOD content SOD significantly increased equally in the EG-50 and EGA-50 groups of rats, compared to the C1 group. In rats in the EG-100 and EGA-100 groups, the SOD content decreases, and in the case of the introduction of untreated GdYVO NPs, the degree of decrease in the enzyme content is significantly higher. In rats in the EG-200 and EGA-200 groups, an even more pronounced and significant decrease in SOD content is observed compared to the control group, and in the EGA-200 group, the decrease in the enzyme content is more pronounced than in

the EG-200 group. Equally important for characterizing the state of the antioxidant system in the liver is the study of the content of reduced glutathione, reflecting the state of the glutathione system. The results of the study of the reduced glutathione in liver homogenates from experimental rats are presented in Table 3. As can be seen from the data we obtained, in the group of rats EG-50 and EGA-50, the reduced glutathione is significantly higher than in the control group. In the rat groups, the content of SH-glutathione EG-100 and EGA-100 is lower than in the control, and in EG-100 is significantly lower than in gr. EGA-100. The same dependence is typical for the EG-200 and EGA-200 groups. Consequently, UV-irradiated and untreated NPs (to a greater extent), administered at a low dose (50 μ g/kg), have restorative properties, increasing the adaptive potential. At higher doses, untreated GdYVO4 NPs do not exhibit reducing properties, while UV-irradiated NPs exhibit pro-oxidant properties. To assess possible damage to the endothelium in the presence of intoxication, the concentration of vWF was studied (Table 4).

Table 4. Content of Willibrandt factor (vWF), indirect (IB), and direct (DB) bilirubin in rat blood serum during oral administration of colloidal solution of GdYVO4: Eu³⁺ NP (in untreated and UV-irradiated form), [Me (25, 75)]*

Groups/Indicators	vWF, ng/ml	IB, μ M/l	DB, μ M/l
Gr. Cl	4.79 [4.62; 4.94]	9.85 [9.35; 10.23]	2.79 [2.63; 2.86]
Gr. EG-50	5.04 [4.89; 5.35] $p_1=0.0931$	9.92 [9.67; 10.19] $p_1=0.270$	2.03 [1.97; 2.08] $p_1=0.0058$
Gr. EGA-50	6.05 [5.84; 6.19] $p_1=0.0022$ $p_2=0.0022$	11.15 [11.03; 11.27] $p_1=0.0055$ $p_2=0.0034$	1.82 [1.78; 1.97] $p_1=0.0035$ $p_2=0.0045$
Gr. EG-100	13.97 [13.72; 14.06] $p_1=0.0022$	13.05 [12.96; 13.17] $p_1=0.0025$	1.88 [1.79; 1.94] $p_1=0.0032$
Gr. EGA-100	17.16 [17.13; 17.46] $p_1=0.0022$ $p_2=0.0022$	14.55 [14.12; 14.67] $p_1=0.0022$ $p_2=0.0034$	1.72 [1.68; 1.81] $p_1=0.0022$ $p_2=0.0022$
Gr. EG-200	34.50 [34.41; 34.72] $p_1=0.0022$	15.98 [15.47; 16.22] $p_1=0.0022$	1.52 [1.44; 1.59] $p_1=0.0019$
Gr. EGA-200	49.08 [48.97; 49.31] $p_1=0.0022$ $p_2=0.0022$	16.59 [16.22; 17.08] $p_1=0.0019$ $p_2=0.0043$	1.43 [1.39; 1.48] $p_1=0.0018$ $p_2=0.0035$

* p_1 – probability of differences between control and experimental groups, p_2 – probability of differences between untreated and UV irradiated groups within one dose

At the application of only UV-irradiated NP at a dose of 50 $\mu\text{g}/\text{kg}$, there is a significant increase in the content of FVB compared to the animals of the control group. At doses of 100 $\mu\text{g}/\text{kg}$ and 200 $\mu\text{g}/\text{kg}$, significant dose-dependent differences in vWF content between the control and experimental groups of rats, as well as between the untreated and UV-irradiated groups within the same dose-dependent differences. The data obtained by us indicate that endothelial dysfunction is significantly expressed in rats when NPs are administered both UV-irradiated and untreated at doses of 100 and 200 $\mu\text{g}/\text{kg}$, to a greater extent when using UV-irradiated GdYVO NPs. At a dose of 50 $\mu\text{g}/\text{kg}$ endothelial dysfunction develops only when UV-irradiated NPs are used.

It is known that one of the most important functions of the liver is the conversion of toxic indirect bilirubin (IB) into nontoxic, water-soluble bilirubin diglucuronide (direct bilirubin, DB). In this regard, in order to evaluate the detoxifying function of rat liver during administration of untreated and UV-irradiated GdYVO NP, we studied the content of DB and IB in the blood serum of experimental rats. The IB content in the blood of the group of rats (EG-50) practically does not differ from the level of the control group, and in the EGA-50 group it was significantly higher than in the control group. In the EG-100 and EGA-100 groups IB concentration is significantly higher than in the control group, and in the EGA-100 group of rats it is significantly higher than in the EG-100 group. The same character of changes, but more pronounced, is observed in groups EG-200 and EGA-200. The DB content in rats of groups EG-100 and EGA-100 groups is significantly lower than in the control group, and in rats of the EGA-100 gr. rats it is significantly lower than in rats of the EG100 gr. are established between the DB content in the control group of rats and in the groups of rats EG-200 and EGA-200. As can be seen from a data obtained by us, the dose-dependent increase in the IB content with a decrease in the DB content is observed during the introduction of GdYVO NPs, especially in the case of UV-activated NPs. The data obtained indicate that the introduction of NPs (particularly UV-irradiated) leads to a decrease in the conjugation process, which is obviously associated with a decrease in the activity (or content) of the conjugation enzyme UGT-glucuroniltransferase and indicates a decrease in the detoxification function of the liver and impaired hepatocyte integrity. Thus, the biochemical assays used in this study showed dose-dependent intoxication of the body, the development of oxidative stress in the liver, and the activity of the GdYVO NPs was enhanced by preliminary activation (UV-irradiation). The circulation of NPs in the bloodstream leads to a dose-dependent death of the vascular endothelium. Furthermore, the entry of NPs from the intestine through the portal system \times to the liver led to an increase in the content of NPs against the background of a decrease in the content of DB in the blood serum.

Morphological studies

The morphological study of liver tissue allowed to confirm pathological metabolic changes. In intact animals (C1 gr.) the lobular structure of the liver, with well visible beams of hepatocytes well-visible beams

of hepatocytes, with correct, id est not altered placement of triads and central veins. The space around the triads (periportal space) has no leukocytic infiltrates. Central veins do not have a collagen layer in the wall. At the same time in the central vein and surrounding sinusoids there is a varying degree of marked hemorrhage, probably due to extinction of the cardiac function during slaughter and the development of general venous hemorrhage. The nuclei of the hepatocytes are light-colored, with small clumps of chromatin, and the cytoplasm in the periportal zone darker than in the area around the central vein (Fig. 2). In microdissections stained with gallocyanin-chromic alum according to Einarson (histochemical staining for nucleic acids), cytophotometry was performed. Cytophotometric determination of the optical density of hepatocyte cytoplasm in the intermediate zone of the liver lobe: $Dk=0.226\pm0.018$ CU of optical density, which can be considered as an indicator of the level of RNA present in the cytoplasm. Sinusoids are lined by endothelium with dark, flat nuclei, the presence of Kupffer cells is moderate.

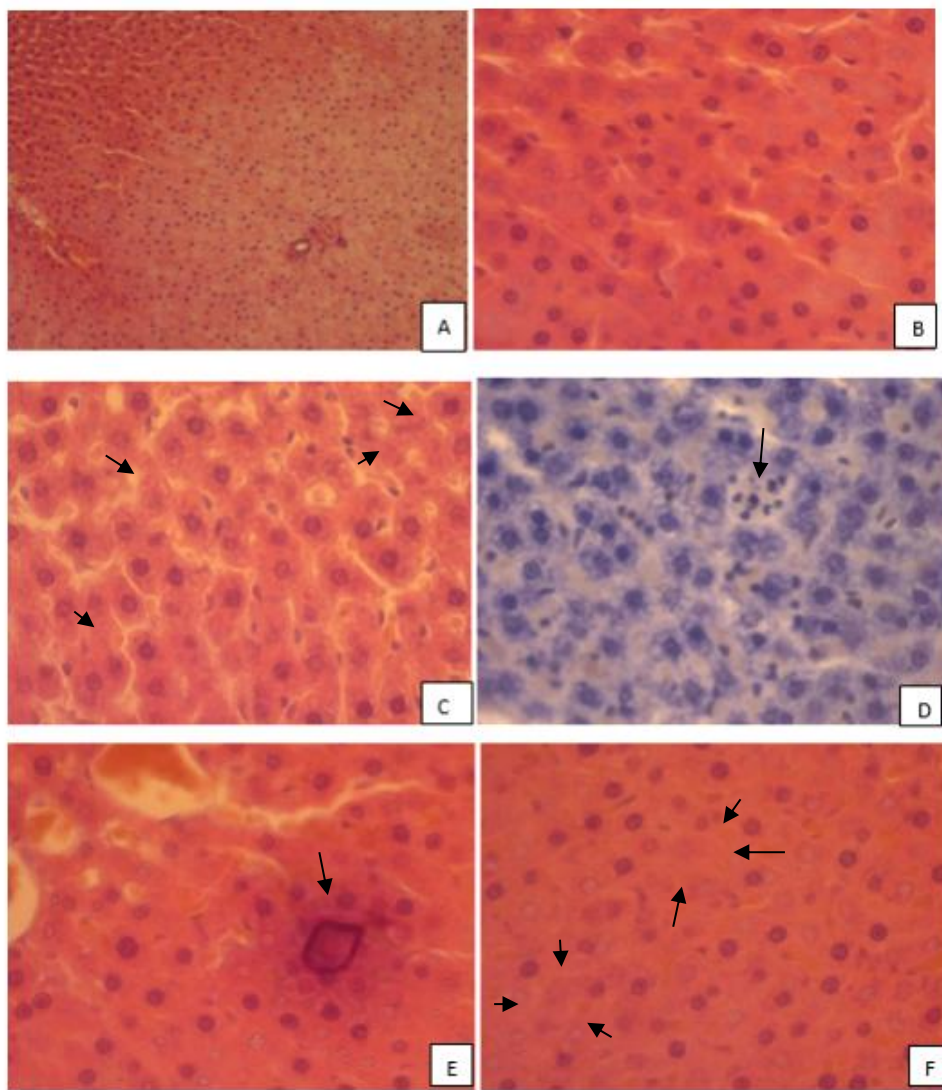


Fig. 2. Microslides of the liver routinely stained with hematoxylin and eosin (A, B, C, E, F), Einarson's gallocyanin stain (D). A: Control group – well-preserved liver histostructure; periportal infiltrate is absent

($\times 100$); B: Control group - In the 2nd zone nuclei of hepatocytes are light colored, euchromic and moderately heterochromic, the cytoplasm is eosinophilic, non-vacuolated ($\times 400$); C: Gr. EG-50 - In the 2nd zone of acinus many small focuses with full karyolysis of hepatocytes, functioning hepatocytes have larger and lighter nuclei, the cytoplasm is non-uniformly eosinophilic, lower number of sinusoids endotheliocytes of sinusoids ($\times 400$); D: Gr. EGA50 – a small focus of necrosis with neutrophil infiltrate of neutrophils ($\times 400$); E: Gr. EG-100 - small petrification in the necrosis zone ($\times 400$); F: Gr. EG-100 - Hepatocytes in the 2nd zone with a significant decrease in the number of sinusoid endotheliocytes and collapse of sinusoids

In animals, which received a course of GdYVO NP at the minimum dose (EG-50 gr.), the histological picture of the appearance of signs of minimal damage to liver tissue, which is accompanied by regeneration and increase in its morpho-functional activity. Namely: in the intermediate (2nd) zone of liver acinuses, there are found areas with absence or decrease in the number of endotheliocytes and Kupffer cells in the lining of sinusoids (Fig. 2). In these areas, hepatocytes have a dark pyknotic nucleus. In other parts of this zone, there is an increase in the number of endotheliocytes and Kupffer cells in the lining of the sinusoids, and hepatocytes, respectively, with a larger nucleus and a higher RNA content in the cytoplasm.

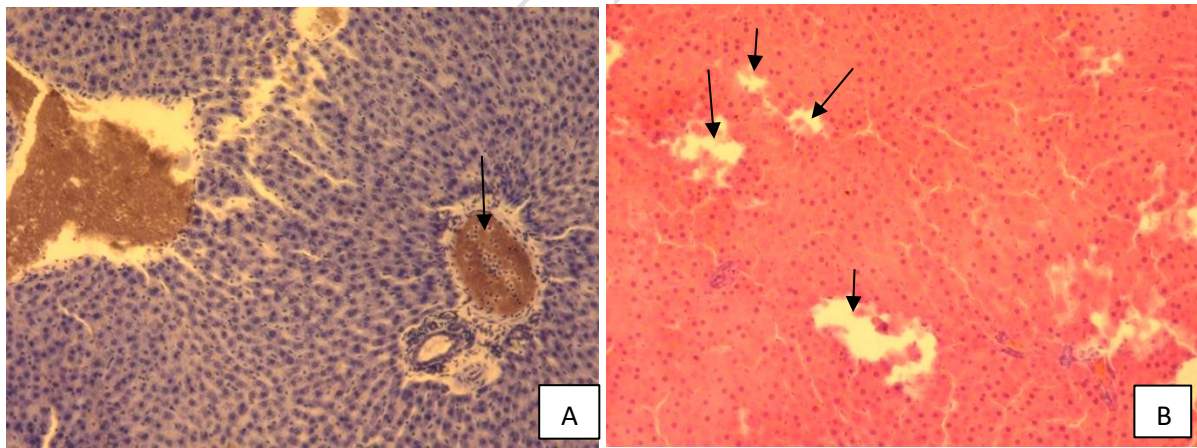
When staining micropreparations with gallocyanin-chromium alum according to Einarson, the average optical density of the hepatocyte cytoplasm in this zone of the liver lobules is less than in C1 gr. (Fig.4). It was possible to detect a section of the sinusoid where an endothelial "kidney" was formed as a result of endotheliocyte proliferation to replenish the dead endothelial lining of the sinusoid (Fig. 2). The periportal space is somewhat expanded with the appearance of minimal leukocyte infiltration. The central veins and adjacent sinusoids are full-blooded to a greater extent than in C1 gr., in some places the endothelial cover of the central veins is desquamated.

In EGA-50 gr. the damage to the endothelium of sinusoids and hepatocytes in the intermediate zone of the liver lobes is noticeably more pronounced, small areas of hepatocyte death appear similar to the area occupied by 3-5 nearby hepatocytes. At complete lysis, these hepatocytes forms a very small pseudocyst, with a few leukocytes. On micro drugs stained with gallocyanin-chromic alum, the focal decrease in RNA content in the cytoplasm of hepatocytes in the intermediate zone and the focal increase, obviously, in young regenerated hepatocytes. When micro-drugs are staining with gallocyanin-chromic alum by Einarson, the average value of optical density of hepatocyte cytoplasm in this zone of the hepatic lobules is unreliable lower than in gr. C1 and unreliable differs from the value of this index in experimental groups of this index in EG-50 (Fig. 4). A small leukocytic infiltrate is observed in the periportal spaces. Additionally, there is more pronounced chromatin margination in the nuclei of hepatocytes located in the zone around the central vein, which is a sign of apoptosis vein, which is a sign of apoptosis.

When animals receive a daily dose of GdYVO NPs 100 μ g/kg (EG-100) liver damage increases compared to EG-50 gr.: in the 2nd zone the areas dominate, where sinusoids collapsed due to the absence of

endothelium and Kupffer cells and therefore such areas look like continuous complexes of hepatocytes without bar structure (Fig. 3). The nuclei of these hepatocytes are dark and hyperchromic, and the cytoplasm has a reduced RNA content. When staining micro-preparations with gallocyanin-chromium alum according to Einarson, the average optical density of the cytoplasm of hepatocytes in this zone of the liver lobules is significantly less than in 1 gr. There is a small infiltration in the periportal spaces, and fullness is present not only in the central veins, but also in the branches of the portal vein, where venous blood contains a large amount of leukocytes.

In EGA-100 gr., the damage to the sinusoid lining and hepatocytes is stimulated so much compared to gr. stimulated, as compared to EG-100 gr, that numerous small pseudocysts are formed in the liver tissue in the same location, numerous small pseudocysts are formed in the hepatic tissue in the same localization, resulting from the death of groups of hepatocytes. The absence of leukocytes around the perimeter of these pseudocysts is noteworthy, indicating that the foci of hepatocyte death are likely to be formed by apoptosis rather than necrosis. Small periportal leukocytic infiltrates are combined with bile duct hyperplasia (3-4). Obviously, hepatocyte death is so intensive that the reparative potential of young hepatocytes in the periportal zone is insufficient, and figures of hepatocyte mitosis are found in the central parts of the space between the central vein and the triad. When staining microdissections Einarson Gallocyanin-Chrome Alum average value of the optical density of cytoplasm of hepatocytes in this hepatic lobule zone was higher than in C1 gr. and in EG100 gr. (Fig. 4), probably caused by the general decrease in the number of hepatocytes in the second zone and compensatory activation of the morphofunctional state of working hepatocytes.



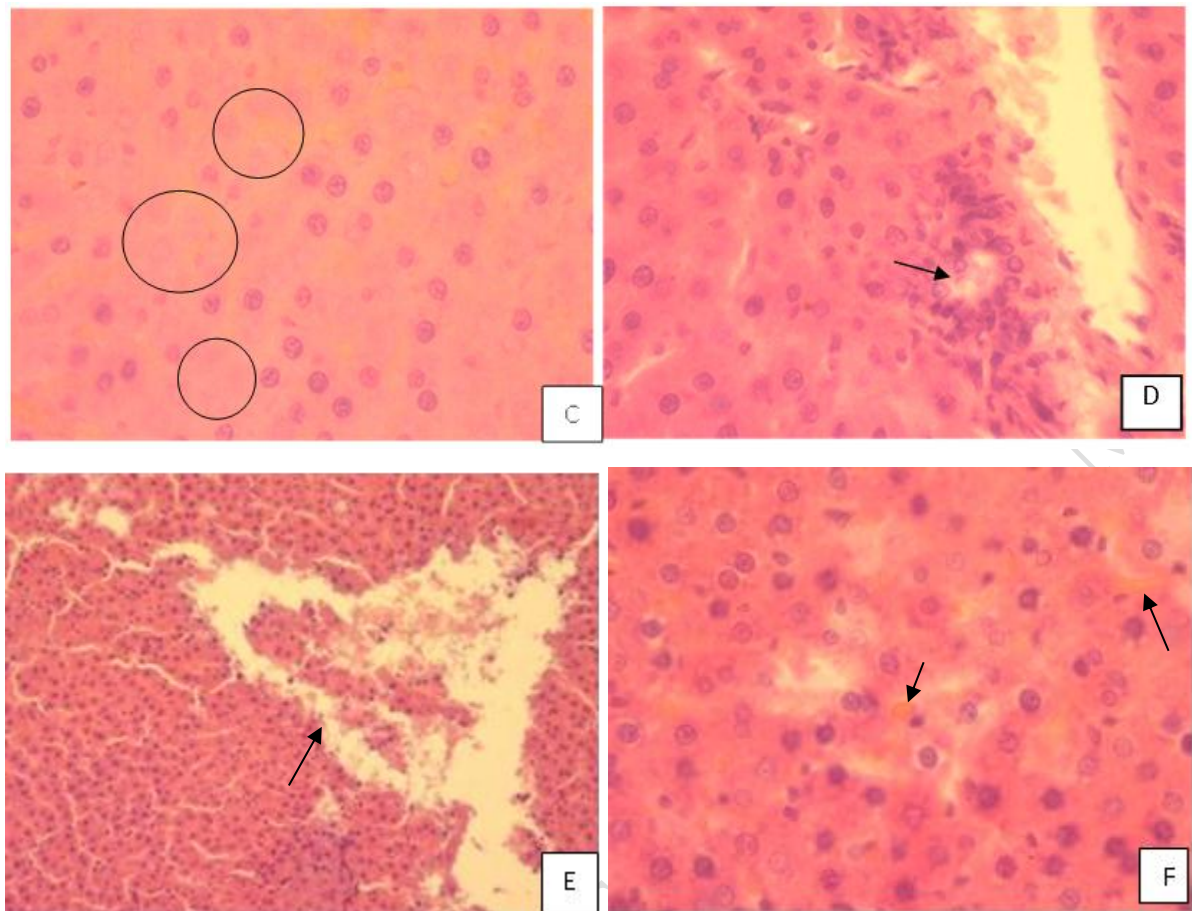


Fig. 3. Microslides of the liver routinely stained with hematoxylin and eosin (B, C, D, E, F), Einarson's gallocyanin stain (A), A: Gr. EG-100 – reduction in trabeculae, large number of leukocytes in blood in a branch of v. portae ($\times 100$); B: Gr. EGA-100 – presence of several small pseudocysts in the second zone sites ($\times 100$); C: Gr. EG-200 – mosaic picture of the death of small groups of hepatocytes with signs of karyolysis ($\times 400$); D: Gr. EGA-200 – inflammation of a biliary duct in the triad, partial destruction of its wall by an infiltrate ($\times 400$); E: Gr. EGA-200 – a large pseudocyst with dead hepatocytes not yet lysed in the lumen ($\times 100$); F: Gr. EGA-200 – parallel to hepatocyte destruction, dilatation of biliary capillary dilation with cholestasis is observed ($\times 400$)

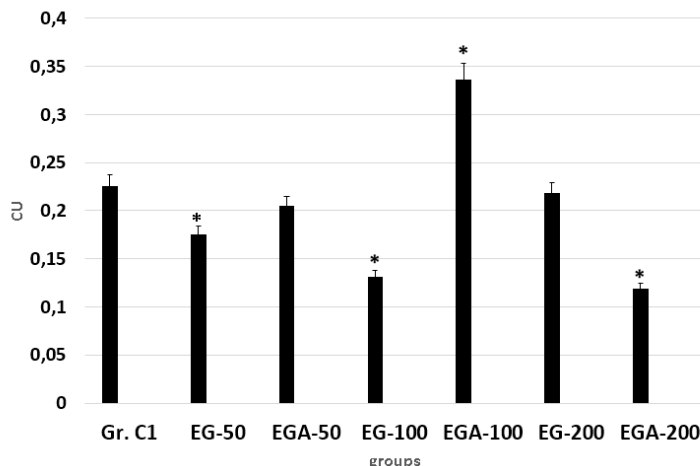


Fig. 4. Optical density of hepatocyte cytoplasm (conditional units, CU) during oral administration of colloidal solution of GdYVO4: Eu³⁺ NP (in untreated and UV-irradiated forms), each group compared to the control group, * – p <0.05

In animals that received the maximum daily dose (EG-200 gr), hepatocytes die even more intensely than in EG-100. Frequent areas of liver tissue, mainly in the intermediate zone, where the trabecular structure is absent, which means that sinusoids have "lost" endothelial lining and collapsed, and hepatocytes in the form of groups of different sizes are in a state of karyolysis (Fig. 3). The optical density of the cytoplasm of functioning hepatocytes in micro-drug staining according to Einarson, in comparison with EG-100 gr. compared to EG-100 gr, is reliably higher, which can also be conditioned by the higher morphofunctional activity of such hepatocytes, which, obviously, has a compensatory significance. The consequence of the focal death of hepatocytes without adequate regeneration is the convergence of triads and central veins. Periportal space with leukocytic infiltrate, increased number of bile ducts. In EGA-200 gr. pseudocysts are more numerous and larger. In the preserved sinusoids there are many lymphocytes and macrophages. Hepatocytes have cytoplasm with a very low RNA content: the optical density of the cytoplasm at Einarson staining is 0.119 ± 0.021 CU of optical density, that is, in these conditions there is a decompensation of the ability of functioning hepatocytes to synthesize RNA. The periportal space has even more pronounced leukocytic infiltration. The wall of the bile duct in the portal tract can be segmentally infiltrated and practically destroyed by leukocytes. In this way, the morphological analysis also confirmed a dose-dependent hepatic tissue lesion induced by GdYVO4:Eu³⁺ NPs, with the damage further enhanced by UV-activated NPs.

Discussion

Recently, nanomaterials with controllable pro and antioxidant properties have attracted considerable attention as a novel therapeutic approach for various diseases, including cancer.³⁹ Among them, GdYVO4:

Eu^{3+} + nanoparticles (GdYVO NPs) with tunable redox activity appear particularly promising for anticancer applications due to their ability to modulate toxicity.^{17-19,27,28} At the microscopic level, the enhanced toxicity of UV-irradiated GdYVO NPs can be attributed to their photocatalytic properties. Specifically, UV exposure induces the generation of electron–hole pairs.^{27,28} In nanoparticles with a high density of structural defects, these defects act as traps for photoinduced charge carriers, allowing them to accumulate. Over time, trapped carriers migrate to the surface of the nanoparticle, where they interact with oxygen and water molecules, producing ROS such as O_2^- and $\cdot\text{OH}$, a phenomenon referred to as “dark ROS generation”^{27,28} Furthermore, it has been shown that UV pre-treatment of GdYVO NPs leads to partial reduction of Eu^{3+} to Eu^{2+} .¹⁸ Electrons stored in Eu^{2+} can subsequently drive ROS production even in the absence of light.¹⁸ Furthermore, the ultrasmall size of GdYVO NPs (~ 2 nm) may further influence their cellular internalization and subcellular interactions, thus contributing to their cytotoxic effects.^{23,40}

The objective of our study was to assess the risk of toxic liver damage with oral administration of a colloidal solution of NPs depending on the dose and UV irradiation. Our investigation of MM in the blood serum of experimental rats revealed a significant increase in content, particularly in groups subjected to doses of 100 and 200 $\mu\text{g}/\text{kg}$ (EG-100, EGA-100, EG-200 and EGA-200). In particular, this increase was more pronounced in groups where NPs were irradiated with UV light at these doses. Surprisingly, even in the EG-50 and EGA-50 groups, a substantial increase in MM content was observed. These findings suggest a dose-dependent intoxication in rats. It is plausible that toxicity is associated not directly associated with NPs themselves, but rather with their complexation with proteins.²⁵⁻²⁶ Investigation of ALT activity in blood has revealed that the introduction of NPs GdYVO₄:Eu³⁺ into the organism induces a dose-dependent increase in hepatocyte membrane permeability. Specifically, within the EG-50 and EGA-50 groups of rats, no discernible disturbance in permeability was observed. On the contrary, within the EG-100 and EGA-100 groups, a notable increase in permeability was detected. The most substantial increase, surpassing the values observed in the control group, was observed in the EG-200 and EGA-200 rat groups. More pronounced disorders are observed in rats injected with activated NPs, which may be the cause of structural and metabolic disorders in the liver. Microscopic examination of hepatic tissue revealed toxic damage to hepatocytes, primarily concentrated in the intermediate zone of the liver lobule–where venous blood from the gastrointestinal tract enters the sinusoids through the v. portae system. The intensity of hepatocyte damage is significantly with the dose of NPs administered to the animals. In the EG-50 group, this damage is characterized by areas with pyknotic nuclei and weak histochemical staining of the cytoplasm for RNA. In contrast, in the EG-200 group, the damage is more severe, manifesting itself as large pseudocysts formed during the course of the experiment. These pseudocysts likely result from the utilization of the cytoplasm, indicating the death of hepatocytes. Preliminary UV activation of NPs at all doses administered led to more pronounced damage to hepatocytes. The degree of destruction in liver tissue across all main groups, including the EGA groups, aligns with the concurrent increase in the content of MMM and ALT activity

in serum. As described above, HP intake of HPs into the organism does not exclude the possibility of activation of the peroxidation process.¹⁹ The data obtained by us indicate that in oral administration of colloidal solution of GdYVO₄:Eu³⁺ in groups of rats EG-100, EGA100, EG-200 and EGA-200 showed a dose-dependent increase in the content of LPO products against the background of decreased content of SOD and glutathione (the main components of the antioxidant system) which indicates the development of oxidative stress. The development of oxidative stress is more pronounced when NPs is administered at a dose of 200 µg/kg. Among the EG-50 and EGA-50 groups, the development of oxidative stress, apparently, is prevented by increasing AOS activity. It should be noted that we revealed an interesting fact: only when nanoparticles are administered at a dose of 50 µg/kg, UV-irradiated and, to a greater extent, untreated NPs have pronounced antioxidant properties. According to data of other researchers, obtained by the introduction of similar NPs but do not have in their yttrium composition, pronounced antioxidant properties are observed even in oral administration in doses of 200-300 µg/kg for 20 days.⁴¹ Apparently, the composition of NPs significantly affects both their adhesive properties and the redox potential of the system.⁴²

Morphologically, we have also confirmed the “unfolding” of both intracellular and cellular regeneration of hepatocytes in response to their destruction. In the EG-50 group, many hepatocytes emerge around foci containing dying hepatocytes, characterized by larger and lighter-colored nuclei. A comparative analysis of the cytophotometrically determined RNA content in the hepatocyte cytoplasm (III.2) prompts us to explore the unexpectedly high level of RNA in the EGA-100 group, surpassing that of the EG-100 group. Examination of liver micropreparations in the intermediate zone of the lobe reveals that in the EGA-100 group, there are relatively few hepatocytes in a wild-type state compared to the EG-100 group. However, pseudocysts are larger and more frequent. Consequently, it can be argued that preirradiation of NPs administered in a high dose enhances the process of hepatocyte death and dystrophy. The remaining 'healthy' hepatocytes work more intensively, leading to a higher RNA content in the cytoplasm. At the maximum dose of nanoparticles in the EGA-200 group, dystrophic hepatocytes dominate among the remaining cells. Therefore, the RNA content in these hepatocytes is lower than in the EG-200 group. It is known that intoxication, the presence of oxidative stress, and direct contact of NPs with endotheliocytes are risk factors for endothelial damage.⁴³⁻⁴⁵ As described above, a dose-dependent increase in the vWF content in the blood was revealed in all rats' groups (except for EG-50 gr.), more pronounced in rats in the EGA groups. Consequently, endothelial damage endsothelium damage occurs in rats of all groups except EGA. The maximum damage is in the rats EGA-200 group. Morphological examination revealed that in all major groups, the endothelium of the sinusoids and the arteries of the portal tract was severely damaged and desquamated. Only in EG-50 gr. there is an active proliferation of endotheliocytes in parallel, which corresponds to the data of the biochemical study on the content of vWF in blood serum. The analysis of bilirubin fractions revealed a dose-dependent increase in the content of IB against the background of DB

decrease, to a greater extent at the introduction of activated NPs, which indicates a decrease in the activity or amount of UDP-glucanoyltransferase, integrity of hepatocyte membranes. The violation of bile production was revealed morphologically: At the application of doses of 100 and 200 $\mu\text{g}/\text{kg}$ there is observed proliferation of bile ducts is observed in "triads", which is a compensatory mechanism in the compensatory mechanism in biliary hepatitis and biliary cirrhosis of the liver. The presence of oxidative stress, intoxication, endotheliocyte damage, membrane permeability disorders, hepatocyte destruction, decreased DB production and destruction of sinusoidal endotheliocytes allows us to assume that in the liver dose-dependent structural and metabolic disorders develop in the liver (EG-50 EG-100 g. EG-200). At the minimal dose of 50 $\mu\text{g}/\text{kg}$, the structural and metabolic disorders are fully compensated. UVa NPs lead to increase of the level of structural-metabolic disorders in liver tissue ($\text{EGA50} \leq \text{EGA-100} \leq \text{EGA-200}$), which is also shown biochemically and morphologically.

Conclusion

The colloidal solution of $\text{GdYVO}_4:\text{Eu}^{3+}$ NPs, UV irradiated to a greater extent, has a pronounced dose-dependent toxicity when administered to rats at the doses studied for 14 days.

The administration of colloidal $\text{GdYVO}_4:\text{Eu}^{3+}$ NPs to rats at doses of 100 and 200 $\mu\text{g}/\text{kg}$ body weight is accompanied by the development of oxidative stress, which is most pronounced for UV-irradiated NPs.

Intoxication, the development of oxidative stress, and direct contact of the nanoparticles with the endothelium contribute to the development of dose-dependent endothelial dysfunction, especially for UV-irradiated NPs, as evidenced by the increase in the concentration of vWF, maximally expressed at a dose of 200 $\mu\text{g}/\text{kg}$.

The increase in the activity of the indicator enzyme AIAT in blood serum and decrease in the DB level on the background of increased IB (most pronounced at administration of untreated and UV-irradiated NPs at a dose of 200 $\mu\text{g}/\text{kg}$ of weight) testify about functional disorders (detoxification function) in the liver.

The data obtained by us allow us to conclude that colloidal solution of $\text{GdYVO}_4:\text{Eu}^{3+}$ NP at oral administration to rats in doses of 100 and 200 $\mu\text{g}/\text{kg}$ of weight for 14 days can induce cell apoptosis mediated by the development of oxidative stress and significant damage to endothelium vessels. The possible therapeutic effect in cancer treatment will be accompanied by significant morphologic and functional liver damage, which requires the use of hepatoprotectors.

When administering colloidal solution of $\text{GdYVO}_4:\text{Eu}^{3+}$ NP at a dose of 50 mcg / kg weight, no significant changes in the parameters were not revealed.

Acknowledgments

The authors thank KhNMU (Kharkiv National Medical University) for support.

Declarations

Funding

The study was supported by the Ukrainian Ministry of Health using the funds provided by the state budget as a fragment of a research entitled ‘Research of Efficiency, Mechanisms of Action and Safety of Use of Orthovanadate Nanoparticles of Rare Earth Elements for Optimization of Radiation Therapy in the Conditions of Oncopathology’ (state registration number 0121U110920).

Author contributions

Conceptualization, O.N., and G.G-V.; Methodology, T.G. and S.S.; Software, I.V.; Validation, V.M. and O.N.; Formal Analysis, D.Y.; Investigation, I.V. and D.Y.; Resources, O.N.; Data Curation, S.D.; Writing – Original Draft Preparation, T.G., S.D; Writing – Review & Editing, O.N., S.Y., V.K. and G.G-V.; Visualization, S.D.; Supervision, S.D. and G. G-V; Project Administration, V.M.; Funding Acquisition, O.N.

Conflicts of interest

The authors declare no competing interests.

Data availability

The data supporting the findings of this study are available from the corresponding author upon reasonable request.

Ethics approval

The study protocol was approved by the Ethics Committee of Kharkiv National Medical University (protocol No. 5; 09.17.2019).

References

1. Raj S, Khurana S, Choudhari R, et al. Specific targeting cancer cells with nanoparticles and drug delivery in cancer therapy. *Semin Cancer Biol.* 2021;69:166-177. doi:10.1016/j.semcancer.2019.11.002
2. Yetisgin AA, Cetinel S, Zuvin M, Kosar A, Kutlu O. Therapeutic Nanoparticles and Their Targeted Delivery Applications. *Molecules.* 2020;25(9):2193. doi:10.3390/molecules25092193
3. Thakur N, Thakur S, Chatterjee S, Das J, Sil PC. Nanoparticles as Smart Carriers for Enhanced Cancer Immunotherapy. *Front Chem.* 2020;8:597806. doi:10.3389/fchem.2020.597806
4. Pavelić K, Kraljević Pavelić S, Bulog A, et al. Nanoparticles in Medicine: Current Status in Cancer Treatment. *Int J Mol Sci.* 2023;24(16):12827. doi:10.3390/ijms241612827

5. Abdesselem M, Schoeffel M, Maurin I, et al. Multifunctional rare-earth vanadate nanoparticles: luminescent labels, oxidant sensors, and MRI contrast agents. *ACS Nano*. 2017;8(11):11126-11137. doi:10.1021/nn504170x
6. Howard D, Sebastian S, Le QV-C, Thierry B, Kempson I. Chemical Mechanisms of Nanoparticle Radiosensitization and Radioprotection: A Review of Structure-Function Relationships Influencing Reactive Oxygen Species. *Int J Mol Sci*. 2020;21(2):579. doi:10.3390/ijms21020579
7. Liu Y, Zhang P, Li F, et al. Metal-based NanoEnhancers for Future Radiotherapy: Radiosensitizing and Synergistic Effects on Tumor Cells. *Theranostics*. 2018;8(7):1824-1849. doi:10.7150/thno.22172
8. Jackson N, Cecchi D, Beckham W, Chithrani DB. Application of High-Z Nanoparticles to Enhance Current Radiotherapy Treatment. *Molecules*. 2024;29(11):2438. doi:10.3390/molecules29112438
9. Ge H, Wang D, Pan Y, et al. Sequence-Dependent DNA Functionalization of Upconversion Nanoparticles and Their Programmable Assemblies. *Angew Chem Int Ed Engl*. 2020;59(21):8133-8137. doi:10.1002/anie.202000831
10. Shi J, Yang X, Li Y, et al. MicroRNA-responsive release of Cas9/sgRNA from DNA nanoflower for cytosolic protein delivery and enhanced genome editing. *Biomaterials*. 2020;256:120221. doi:10.1016/j.biomaterials.2020.120221
11. Bakshi S, Zakharchenko A, Minko S, Kolpashchikov DM, Katz E. Towards Nanomaterials for Cancer Theranostics: A System of DNA-Modified Magnetic Nanoparticles for Detection and Suppression of RNA Marker in Cancer Cells. *Magnetochemistry*. 2019;5(2):24. doi:10.3390/magnetochemistry5020024
12. Ahmadzada T, Reid G, McKenzie DR. Fundamentals of siRNA and miRNA therapeutics and a review of targeted nanoparticle delivery systems in breast cancer. *Biophys Rev*. 2018;10(1):69-86. doi:10.1007/s12551-017-0392-1
13. Wang L, Hu C, Shao L. The antimicrobial activity of nanoparticles: present situation and prospects for the future. *Int J Nanomedicine*. 2017;12:1227-1249. doi:10.2147/IJN.S121956
14. Agarwal H, Nakara A, Shanmugam VK. Anti-inflammatory mechanism of various metal and metal oxide nanoparticles synthesized using plant extracts: A review. *Biomed Pharmacother*. 2019;109:2561-2572. doi:10.1016/j.biopha.2018.11.116
15. Tkachenko A, Pogozhykh D, Onishchenko A, et al. Gadolinium Orthovanadate $\text{GdVO}_4:\text{Eu}^{3+}$ Nanoparticles Ameliorate Carragttan-induced intestinal Inflammation *Journal of Pharmacy and Nutrition Sciences*, 2021;11:40-48. doi: <https://doi.org/10.29169/1927-5951.2021.11.06>
16. Yefimova SL, Maksimchuk PO, Seminko VV, et al. Janus-faced redox activity of $\text{LnVO}_4:\text{Eu}^{3+}$ ($\text{Ln} = \text{Gd, Y, and La}$) nanoparticles. *J Phys Chem C*. 2019;123(24):15323-15329. doi.org/10.1021/acs.jpcc.9b03040

17. Maksimchuk PO, Hubenko KO, Grygorova GV, Klochkov VK, Sorokin AV, Yefimova SL. Impact of Eu³⁺ ions on prooxidant activity of ReVO₄ : Eu³⁺ nanoparticals. *J Phys Chem C*. 2021;125(2):1564-1569. doi.org/10.1021/acs.jpcc.Oc10028

18. Maksimchuk PO, Yefimova SL, Omielaieva VV, et al. X-ray Induced Hydroxyl Radical Generation by GdYVO₄:Eu³⁺ Nanoparticles in Aqueous Solution: Main Mechanisms. *Crystals*. 2020;10(5):370. <https://doi.org/10.3390/crust10050370>

19. Anselmo AC, Mitragotri S. Nanoparticles in the clinic: An update. *Bioeng Transl Med*. 2019;4(3):e10143. doi:10.1002/btm2.10143

20. Kasi PB, Mallela VR, Ambroziewicz F, Trailin A, Liška V, Hemminki K. Theranostics Nanomedicine Applications for Colorectal Cancer and Metastasis: Recent Advances. *Int J Mol Sci*. 2023;24(9):7922. doi:10.3390/ijms24097922

21. Davies J, Siebenhandl-Wolff P, Tranquart F, Jones P, Evans P. Gadolinium: pharmacokinetics and toxicity in humans and laboratory animals following contrast agent administration. *Arch Toxicol*. 2022;96(2):403-429. doi:10.1007/s00204-021-03189-8

22. Radulescu DM, Surdu VA, Ficai A, Ficai D, Grumezescu AM, Andronescu E. Green Synthesis of Metal and Metal Oxide Nanoparticles: A Review of the Principles and Biomedical Applications. *Int J Mol Sci*. 2023;24(20):15397. doi:10.3390/ijms242015397

23. Khan I, Saeed K, Nanoparticles properties? Applications and toxicitts. *Arabian Journal of Chemistry* 2019;12(7):908-931 doi:10.1016/j.arabjc.2017.05.0

24. Sun H, Jiang C, Wu L, Bai X, Zhai S. Cytotoxicity-Related Bioeffects Induced by Nanoparticles: The Role of Surface Chemistry. *Front Bioeng Biotechnol*. 2019;7:414. doi:10.3389/fbioe.2019.00414

25. Önal Acet B, Gül D, Stauber RH, Odabaşı M, Acet Ö. A Review for Uncovering the "Protein-Nanoparticle Alliance": Implications of the Protein Corona for Biomedical Applications. *Nanomaterials (Basel)*. 2024;14(10):823. doi:10.3390/nano14100823

26. Maksimchuk P, Yefimova S, Hubenko K, et al. Dark reactive oxygen species generation in ReVO₄:Eu³⁺(Re=Gd, Y) nanoparticles in aqueous solutions. *J Phys Chem C*. 2020;124(6):3843-3850. doi:10.1021/acs.jpcc.9b10143

27. Yefimova SL, Maksimchuk PO, Hubenko KO, et al. Light-triggered redox activity of GdYVO₄:Eu³⁺ nanoparticles. *Spectrochim Acta A Mol Biomol Spectrosc*. 2020;242:118741. doi:10.1016/j.saa.2020.118741

28. Onishchenko A, Myasoedov V, Yefimova S, et al. UV Light-Activated GdYVO₄:Eu³⁺ Nanoparticles Induce Reactive Oxygen Species Generation in Leukocytes Without Affecting Erythrocytes In Vitro. *Biol Trace Elem Res*. 2022;200(6):2777-2792. doi:10.1007/s12011-021-02867-z

29. Weng TI, Chen HJ, Lu CW, et al. Exposure of Macrophages to Low-Dose Gadolinium-Based Contrast Medium: Impact on Oxidative Stress and Cytokines Production. *Contrast Media Mol Imaging*. 2018;2018:3535769. doi:10.1155/2018/3535769

30. Klochkov VK, Malyshenko AL, Sedyh OO, Malyukin YuV. Wet-chemical synthesis and characterization of luminescent colloidal nanoparticles ReVO_4 : Eu^{3+} (Re=La, Gd, Y) with rod- like and spindle-like shape. *Fanctional materials*. 2011;1:111-115.

31. Dzyubanovsky II, Vervega BM, Pidruchna SR, Melnyk NA. Syndrome of endogenous intoxication at experimental peritonitis against the background of diabetes. *Bulletin of Scientific Research*. 2019;1:135-139. doi:10.11603/2415-8798.2019.1.10004.

32. Stoscheck CM. Quantitation of protein. *Methods Enzymol*. 1990;182:50-68. doi:10.1016/0076-6879(90)82008-p

33. Botsoglou NA, Fletouris DJ, Papageorgiou G, et al. Rapid, sensitive, and specific thiobarbituric acid method for measuring lipid peroxidation in animal tissue, food, and feedstuff samples. *Journal of Agricultural and Food Chemistry*. 1994;42(9):1931-1937. doi:10.1021/JF00045A019

34. Cammansky I, Cruener V. Spectrofotometric methods for measuring diene conjugation. *Clin Chem Acta*. 1997;259:177-179

35. Tietze F. Enzymic method for quantitative determination of nanogram amounts of total and oxidized glutathione: applications to mammalian blood and other tissues. *Anal Biochem*. 1969;27(3):502-522. doi:10.1016/0003-2697(69)90064-5

36. Tupper J, Tozer GM, Dachs GU. Use of horseradish peroxidase for gene-directed enzyme prodrug therapy with paracetamol. *Br J Cancer*. 2004;90(9):1858-1862. doi:10.1038/sj.bjc.6601780

37. Zelditch ML, Swiderski DL, Sheets HD, Fink WL. Geometric Morphometrics for Biologists: A Primer. 3rd ed. Elsevier Academic Press; 2012:488 p. ISBN 978-0-12-386903-6

38. Yang B, Chen Y, Shi J. Reactive Oxygen Species (ROS)-Based Nanomedicine. *Chem Rev*. 2019;119:4881-4985. <https://doi.org/10.1021/acs.chemrev.8b00626>

39. Mosquera J, García I, Liz-Marzán LM. Cellular Uptake of Nanoparticles versus Small Molecules: A Matter of Size. *Acc Chem Res*. 2018;51(9):2305-2313. doi:10.1021/acs.accounts.8b00292

40. Nikitchenko YV, Klochkov VK, Kavok NS, et al. Age-Related Effects of Orthovanadate Nanoparticles Involve Activation of GSH-Dependent Antioxidant System in Liver Mitochondria. *Biol Trace Elem Res*. 2021;199(2):649-659. doi:10.1007/s12011-020-02196-7

41. Mundekkad D, Cho WC. Nanoparticles in Clinical Translation for Cancer Therapy. *Int J Mol Sci*. 2022;23(3):1685. doi:10.3390/ijms23031685

42. Xuan L, Ju Z, Skonieczna M, Zhou PK, Huang R. Nanoparticles-induced potential toxicity on human health: Applications, toxicity mechanisms, and evaluation models. *MedComm* (2020). 2023;4(4):e327. doi:10.1002/mco2.327

43. Min Y, Suminda GGD, Heo Y, Kim M, Ghosh M, Son YO. Metal-Based Nanoparticles and Their Relevant Consequences on Cytotoxicity Cascade and Induced Oxidative Stress. *Antioxidants (Basel)*. 2023;12(3):703. doi:10.3390/antiox12030703

44. Huang C, Liu X, Wu Q, et al. Cardiovascular toxic effects of nanoparticles and corresponding molecular mechanisms. *Environ Pollut*. 2024;356:124360. doi:10.1016/j.envpol.2024.124360

45. Xi WS, Tang H, Liu YY, et al. Cytotoxicity of vanadium oxide nanoparticles and titanium dioxide-coated vanadium oxide nanoparticles to human lung cells. *J Appl Toxicol*. 2020;40(5):567-577. doi:10.1002/jat.3926